

N 62 61388

RM E52C25

NACA RM E52C25



# RESEARCH MEMORANDUM

INVESTIGATION OF TURBINES FOR DRIVING SUPERSONIC COMPRESSORS

I - DESIGN AND PERFORMANCE OF FIRST CONFIGURATION

By Warner L. Stewart, Harold J. Schum, and Warren J. Whitney

Lewis Flight Propulsion Laboratory  
Cleveland, Ohio

NATIONAL ADVISORY COMMITTEE  
FOR AERONAUTICS

WASHINGTON

June 17, 1952  
Declassified October 14, 1957

NATIONAL ADVISORY COMMITTEE FOR AERONAUTICS

RESEARCH MEMORANDUM

INVESTIGATION OF TURBINES FOR DRIVING SUPERSONIC COMPRESSORS

I - DESIGN AND PERFORMANCE OF FIRST CONFIGURATION

By Warner L. Stewart, Harold J. Schum, and  
Warren J. Whitney

SUMMARY

The design and performance of a turbine to drive a supersonic compressor are presented in order to determine the problems that would be encountered in turbines required to drive high-speed, high-weight-flow compressors. A 14-inch cold-air model of this turbine was built and operated over a range of speed from 30 percent to 130 percent design speed and over a wide range of total-pressure ratios. The air-inlet temperature and pressure were maintained constant at 135° F and 32 inches of mercury absolute, respectively.

Extremely high centrifugal stresses at the hub of the rotor blades were encountered in the design of the turbine and could be attributed to the high-speed, high-weight-flow characteristics of the compressor. High entrance relative Mach numbers were also encountered at the rotor hub and were decreased to a Mach number of 0.69 by increasing the turbine diameter 8 percent over that of the compressor. To reduce the rotor blade stress a high degree of rotor blade taper was incorporated into the design, resulting in an average rotor blade hub stress of 46,600 pounds per square inch.

In the attempt to decrease the stress at the rotor blade hub by the use of high turbine-exit absolute velocities, an extreme blade taper, and an insweep of the inner wall, a flow area was used within the rotor that proved insufficient to pass the required weight flow. The turbine performance indicated that at design speed 95 percent design weight flow was passed and the desired nozzle-exit tangential velocities were not obtained. An increase in work could therefore be obtained only with negative exit tangential velocities. However, the turbine limiting-loading point was reached at a work slightly less than design.

INTRODUCTION

In recent years compressors have been developed that are capable of utilizing increasingly higher air weight flows per unit frontal area.

In certain types of these compressors, such as the supersonic compressor, the pressure ratio is developed by means of high rotational speeds. The two characteristics of high specific air weight flow and high rotational speeds introduce a severe stress problem in the design of turbines that must drive these compressors. Extremely high stresses that occur at the hub of the rotor blade can be attributed principally to the rotor blade centrifugal forces.

The stress due to centrifugal force can be diminished considerably by introducing a high degree of blade taper into the turbine design (reference 1). If the blade chord as well as the section area must be reduced at the blade tip, it would be expected that additional aerodynamic problems would result from the large solidity variation from hub to tip.

The design, construction, and experimental investigation of a turbine to power a typical high-speed, high specific air-weight-flow compressor were undertaken at the NACA Lewis laboratory to determine the problems that would be incurred in a turbine of this type. In order to define the turbine performance requirements, compressor characteristics were first ascertained. The compressor example chosen was a supersonic compressor designed to operate at a flight Mach number of 1.7 at an altitude of 37,000 feet and to utilize an equivalent weight flow of 30 pounds per second per square foot frontal area at an actual tip speed of 1500 feet per second. The compressor was assumed to develop a pressure ratio of 4 at an adiabatic efficiency of 0.75. Under these conditions the compressor equivalent tip speed was 1362 feet per second. It is recognized that if the engine were designed to operate at constant speed over a range of altitudes and Mach numbers, there could be turbine requirements more critical than those at the conditions specified. However, in this report, the investigation was confined to this altitude and Mach number condition.

While a cold-air model of the turbine designed to operate at the aforementioned conditions was under construction, an analytical investigation of the flow through this turbine rotor was performed. The results are reported in reference 2. This analysis was based on axially symmetric, isentropic flow and indicated that the weight flow as calculated by the reference method was lower than that used in the rotor design. The reduction in weight flow as indicated by the analysis was attributed to the inner-wall profile, the thick blade section at the rotor hub, and the resulting pressure distribution along the orthogonal in combination with the high relative Mach numbers near the blade exit.

The objective of the present report is to present the design of the turbine to drive a supersonic compressor and the experimental performance of a cold-air turbine of this design. The design and aerodynamic problems encountered will also be discussed.

The turbine was operated over a range of speed from 30 to 130 percent design speed and at total-pressure ratios from 1.4 to 2.6. The turbine-inlet temperature and pressure were maintained constant at 135° F and 32 inches of mercury absolute. The performance of this turbine is presented and compared with the design performance. Nozzle-exit static pressures and absolute rotor gas-exit-angle surveys are also included to illustrate the aerodynamic problems encountered in the experimental investigation.

### TURBINE DESIGN

The turbine was designed to drive a supersonic compressor in an engine operating at supersonic flight velocities. The turbine requirements were calculated from the engine operating conditions assuming a turbine-inlet temperature of 2500° R. The first phase of the design was based on a turbine diameter equal to the compressor diameter because of the desirability of low turbine weight and small frontal area. The turbine performance requirements at engine operating conditions, based on equal diameters, can be summarized as follows:

$$\frac{W}{A_F} = 27.4 \text{ pounds per second per square foot frontal area}$$

$$U_t = 1500 \text{ feet per second}$$

$$\Delta h' = 93.7 \text{ Btu per pound}$$

and for an assumed efficiency of 0.80,

$$\frac{p'_1}{p'_3} = 2.10$$

(All symbols used in this report are defined in appendix A.)

When an attempt was made to obtain a turbine design that met these requirements, the problems of high blade stress and high relative Mach number at the rotor blade hub were incurred.

Stress problem. - As indicated by reference 1, the stress at the rotor blade hub (for a blade of constant hub and tip radii) induced by centrifugal force can be expressed by the following equation:

$$s_b = \frac{\rho_m \omega^2 A_a \psi}{288\pi g} = \frac{\rho_m U_t^2 \left[ 1 - \left( \frac{D_h}{D_t} \right)^2 \right] \psi}{288g} \quad (1)$$

Since the initial requirement of equal compressor and turbine diameters had been made, the tip speed and specific air weight flow of the turbine were determined from the compressor requirements.

From equation (1) it can be seen that, for a given blade metal density, the calculated untapered stress could be lowered only by increasing the hub-tip radius ratio of the turbine. However, if the absolute critical velocity ratio  $\frac{V_{x,3}}{V_{cr}}$  of the gas leaving the turbine is 0.7 (which was considered a practical upper limit) and the absolute flow direction is axial, the resulting exit annulus area (and hence the exit hub-tip radius ratio) represents the condition of minimum stress. Under this condition the untapered stress at the exit of the turbine rotor calculated by equation (1) was 96,000 pounds per square inch, assuming a value of 540 pounds per cubic foot as a representative value for blade metal density  $\rho_m$ . This stress as calculated by equation (1) based on the rotor-exit annulus area was prohibitively high and had to be decreased. This decrease was accomplished by introducing an extreme blade taper and by contouring the rotor hub so as to reduce the average blade height. The annulus area and resultant blade height (used in equation (1) to calculate the high stress) are required only at the turbine exit. Consequently, a decrease in the average stress could be made by reducing the average blade height throughout the rotor since a larger hub-tip radius ratio can be used at the inlet than at the outlet, as will be discussed in the following sections. Lowering the stress by schemes such as those discussed, however, could introduce aerodynamic limitations in the turbine. Because of the exit conditions, which were selected from stress considerations, high relative free-stream Mach numbers at the blade outlet would be expected; and the blade would therefore operate at, or near, the choked condition.

Relative Mach number problem. - The rotor-entry velocity diagrams were obtained assuming free-vortex flow ( $V_u = Cr^{-1}$ ) and simple radial equilibrium. The turbine-outlet absolute critical velocity ratio of the gas was set at 0.7 with the flow direction axial, as mentioned in the previous section. The entering Mach number relative to the rotor blade at the hub section was of the order of unity, as shown in the upper curve of figure 1. The high relative Mach numbers occur because of the work output, the high specific weight-flow requirements, and the rotor speed.

In an attempt to reduce the relative Mach number at the rotor blade hub, the effect of varying the turbine diameter from that of the compressor was studied. This effect was investigated maintaining free-vortex distribution and blade-outlet flow conditions as mentioned in the previous section. The resulting entering Mach numbers relative to the rotor at the hub are shown in figure 1 as a function of the rotor hub-tip radius ratio with the ratio of turbine diameter to compressor

diameter as the parameter. It can be seen that for a given diameter ratio, there is a hub-tip radius ratio at which a minimum entering Mach number occurs. At hub-tip radius ratios above this point the relative Mach number is greater because of high axial velocities, while at hub-tip ratios below this point it is greater because of high tangential velocities. This minimum Mach number decreases rapidly as the ratio of turbine diameter to compressor diameter is increased and reaches a practical Mach number value of 0.69 (point A, fig. 1) at a hub-tip radius ratio of 0.70. This represents an 8 percent increase in turbine diameter over compressor diameter.

It can be seen from equation (1) that the untapered stress at the turbine outlet will not change if the turbine diameter is varied from that of the compressor. This occurs because once the compressor size (with corresponding weight flow) and turbine exit conditions have been chosen,  $\omega$  and  $A_a$  at the rotor exit will be fixed.

Consideration of a two-stage turbine. - The feasibility of employing a two-stage turbine for this application was also investigated. The two stages were assumed to produce the same equivalent work and operate with free-vortex flow at the blade inlet and zero tangential velocity at the blade outlet. The flow conditions at the outlet of the second stage were assumed the same as those at the outlet of the single-stage turbine.

The results of this investigation indicate that it is possible to obtain a two-stage turbine with the same tip diameter as that of the compressor for this application. The Mach number relative to the rotor blade at the hub was found to be reasonably low for both stages. The stress problem, however, would not be alleviated because the blade stress at the outlet of the second stage would be the same as that at the outlet of the single stage. Furthermore, the cooling problem would be more severe for the two-stage unit because of the increased blade area exposed to the hot gas.

Selection of turbine design. - In view of the foregoing considerations, the design selected was a single-stage turbine with an increase in blade-tip diameter of 8 percent over that of the compressor. This design is represented in figure 1 by point A. The design utilized free-vortex entry with zero exit tangential velocity and an absolute critical velocity ratio leaving the turbine of 0.7. The blade inlet hub-tip radius ratio was 0.70 (fig. 1). The hub-tip radius ratio at the blade outlet (0.61) was calculated from the aforementioned turbine-outlet flow conditions and the specific air weight flow corresponding to the increased turbine diameter. The untapered stresses at the blade inlet and outlet, as calculated by equation (1), were 78,500 and 96,000 pounds per square inch, respectively.

Design procedure. - The velocity diagrams were obtained for this turbine design assuming isentropic flow through the nozzle blades. A turbine efficiency of 0.80 was assumed to determine the turbine-outlet stagnation state and the required flow area. The design of the turbine blade was based on the tip section and a section at a 0.70 radius ratio. Figure 2 presents the velocity diagrams and side view of the turbine rotor blade with the hub and tip sections shown. At these two sections a mean camber line was drawn to give the blade a positive angle of incidence of  $2^{\circ}$ . The blade shapes were then constructed around these mean camber lines. The blade leading- and trailing-edge radii and the thickness of the tip section were governed by cooling considerations. The tip section was laid out around the mean camber line to obtain a smooth converging blade passage. The hub section was a 12-percent-thick symmetrical airfoil modified for leading- and trailing-edge radii. The cross-sectional area of the rotor blade at the tip was made 30 percent of that at the root, yielding a stress correction factor of approximately 0.52. The hub and tip sections were then stacked and the blade was formed by fairing in straight lines between the two sections. The rotor blade inner wall was formed by fairing a smooth parabolic curve from the hub radius at the rotor inlet to that at the rotor outlet (fig. 2). The stresses calculated as in the preceding section at the blade inlet and outlet would be reduced to 41,000 and 50,000 pounds per square inch, respectively, if the stress correction factor was taken into account.

The stresses were also calculated for the actual blade shape by dividing the blade into strips of elemental axial width. The strips were of uniform width but tapered because of the change in blade thickness from hub to tip. This taper correction was included in the stress calculation. The resulting maximum stress which occurred at an axial station indicated by the dashed line (fig. 2) was 63,500 pounds per square inch, whereas the average stress was 46,600 pounds per square inch. This method is considered to give a better indication of the average blade stress. In the actual blade the elements are not free to deform independently and part of the load of a highly stressed element would be carried by its adjacent less stressed elements. Hence, the actual maximum blade stress would lie between the calculated maximum and the average.

The number of rotor blades was selected from consideration of solidity at the blade hub and tip sections. Twenty-nine blades were used, resulting in hub and tip solidities of 2.2 and 0.8, respectively.

The design of the 32 nozzle blades was also based on the hub and tip sections. These sections were laid out to form smooth converging flow channels. At the tip section the required turning ( $50^{\circ}$ ) was accomplished in the channel. At the hub section the required turning of  $60^{\circ}$  could not be accomplished in the guided channel with the correct

area variation. Accordingly, the flow channel at the hub section was made to converge to a choking throat area, with the additional turning and expansion to be accomplished downstream of this nozzle throat.

The nozzle vane was formed by stacking the two sections so that the centers of the trailing-edge radii formed a radial line and by fairing straight lines between these two sections.

#### APPARATUS AND INSTRUMENTATION

Apparatus. - The turbine used in the experimental investigation was a 14-inch cold-air model of the configuration discussed in the preceding sections. The equivalent turbine requirements discussed in the TURBINE DESIGN section, when corrected for a turbine-to-compressor diameter ratio of 1.083, are as follows:

$$\epsilon \frac{w \sqrt{\theta_{cr}}}{A_f \delta} = 14.2 \text{ pounds per second per square foot}$$

$$\epsilon \frac{w \sqrt{\theta_{cr}}}{\delta} = 15.2 \text{ pounds per second for the 14-inch turbine}$$

$$\frac{U_t}{\sqrt{\theta_{cr}}} = 752 \text{ feet per second}$$

$$\frac{\Delta h'}{\theta_{cr}} = 20.0 \text{ Btu per pound}$$

The equivalent operating conditions ( $\gamma = 1.40$ ) for the 14-inch turbine were obtained from the engine operating conditions ( $\gamma = 1.30$ ) by the method discussed in reference 3. The design adiabatic efficiency of 0.80 and corresponding total-pressure ratio of 2.10 at altitude resulted in an equivalent total-pressure ratio of 2.19.

The 32 nozzle blades were precision cast of aluminum and were held in position by inner and outer shroud bands with diameters of 9.80 and 14.00 inches, respectively. The 29 rotor blades were machined from 24S-T4 aluminum alloy and were hand finished. The rotor blades had a constant tip diameter of 13.94 inches, while the casing inside diameter was 14.00 inches. A photograph of the turbine rotor assembly is presented in figure 3. The low tip solidity, high degree of blade taper, and hub diameter change can be readily noted.

Pressurized air from the laboratory combustion-air system was metered by an adjustable orifice located in a straight section of the inlet ducting. The air was then passed through butterfly throttle valves and through a filter tank in order to remove any foreign particles in the air, and was then ducted into a collector from two opposite sides. Baffles were located in the collector to assure an even flow distribution to the inlet-section annulus preceding the turbine nozzle blades. The collector and baffles can be noted in the diagrammatic sketch of the test section shown in figure 4. In order to obtain a uniform air flow distribution to the blading, the inlet annulus area was decreased by use of a fairing section on the outer diameter of the casing. The air was then passed through the turbine blading, through the outboard bearing support, and finally into the discharge pipe connected to the laboratory altitude-exhaust facilities. Butterfly throttle valves were located in the discharge pipe after the exhaust tank downstream of the rotor.

A 2000-horsepower eddy-current dynamometer was used to absorb the turbine power output. The dynamometer was coupled to the turbine shafting through a step-up gearbox.

Instrumentation. - The air weight flow was metered by a standard calibrated, adjustable, submerged orifice located in a straight section of the inlet ducting.

Turbine-inlet measurements were taken in the annulus preceding the nozzle blading (station 1, fig. 4). Four static-pressure taps were installed  $90^{\circ}$  apart and diametrically opposite on both the inner and outer walls. A total of five bare-wire thermocouples, located at the area centers of equal annular areas, were mounted in the same plane as the static taps.

Four static-pressure taps were located on both the inner and outer nozzle shroud bands immediately downstream of the nozzle blades (station 2, fig. 4) and in approximately the same longitudinal plane as the inlet static-pressure taps. Each of these nozzle discharge pressure taps was centrally located in the projected flow passage between two adjacent blades.

A total-pressure claw probe was mounted on a self-aligning actuator approximately 2 inches downstream of the rotor (station 3, fig. 4) in order to obtain a survey of the absolute air angle leaving the rotor. Eight static taps, four on the inner wall and four on the outer wall, were installed  $90^{\circ}$  apart and in the same axial plane as the total-pressure claw probe.

A thermocouple rake, consisting of five doubly shielded thermocouples, again arranged at the area centers of equal annular areas, was installed in the discharge ducting approximately 4 feet downstream of the rotor (station 4, fig. 4). Inlet and outlet thermocouple rakes were calibrated for recovery factor over a range of Mach numbers corresponding to those encountered in test conditions. The turbine casing was insulated with 2 inches of glass wool between the rotor discharge and the thermocouple rake to reduce the possibility of heat transfer between the working fluid and the ambient air.

All pressures were measured with mercury manometers with the exception of the differential pressure across the orifice, which was measured with a water manometer. Temperatures were taken with calibrated iron-constantan thermocouples and measured with a sensitive calibrated potentiometer in conjunction with a spotlight galvanometer. The speed of the dynamometer was measured with a chronometric tachometer driven by an electric generator geared to the gearbox.

#### PROCEDURE

The turbine was operated at constant inlet conditions of 32 inches of mercury absolute and 135° F. The turbine was operated at constant speed values over a range from 30 through 130 percent design speed in even increments of 10 percent. For each speed investigated, a range of total-pressure ratios from 1.4 to 2.6 was obtained by varying the exhaust pressure from the minimum value possible, as dictated by the capacity of the exhaust facilities, to the maximum pressure where stable operation existed.

#### CALCULATIONS

The turbine was rated on the basis of the ratio of inlet total pressure to an outlet total pressure defined as the sum of the static pressure and the pressure head of the axial component of outlet velocity. The inlet total pressure was calculated from the weight flow, inlet static pressure, and inlet total temperature by the equation (reference 4)

$$p'_1 = p_1 \left[ \frac{1}{2} + \sqrt{\frac{1}{4} + \frac{(r-1)}{2gr} \left( \frac{w}{p_1 A_{a,1}} \right)^2 RT'_1} \right]^{\frac{r}{r-1}} \quad (2)$$

The outlet total pressure, which consisted of the sum of the static pressure and the pressure head of the axial component of outlet velocity, was calculated from the equation (derived in appendix B)

$$p'_3 = p_3 \left[ 1 - \frac{1}{2} \cos^2 \alpha_3 + \frac{1}{2} \sqrt{\cos^4 \alpha_3 + \left( \frac{Rw}{p_3 A_{a,3}} \right)^2 \frac{4T'_4}{K} \cos^2 \alpha_3} \right]^{\frac{r}{r-1}} \quad (3)$$

where  $\alpha_3$  is the average absolute flow angle of the outlet gas measured from the axial direction and  $T'_4$  is the arithmetic average total temperature obtained from the thermocouple rake. The outlet total pressure was calculated for conditions at station 3 by use of the total temperature measured at station 4 (fig. 4). The temperature  $T'_4$  was assumed to be the same as that at station 3. It was believed a more reliable indication of temperature could be obtained at station 4 because (1) the fluctuations of the gas flow out of the rotor would be damped to some extent, and (2) the gas velocity would be considerably lower.

The turbine efficiency was calculated as the ratio of actual enthalpy drop (as obtained from inlet and outlet total temperature) to ideal enthalpy drop as obtained from the inlet total temperature and total-pressure ratio.

The precision of the measured and calculated quantities is estimated to be within the following limits:

Temperature, °R . . . . .	±0.5
Pressure, in. Hg. . . . .	±0.05
Weight flow, percent. . . . .	±1.0
Turbine speed, percent. . . . .	±0.5
Efficiency, percent . . . . .	±2.0

## RESULTS AND DISCUSSION

Over-all performance. - The performance of the experimental turbine is illustrated in figure 5. The equivalent work  $\Delta h' / \theta_{cr}$  as calculated by the temperature measurements is shown as a function of the equivalent weight-flow parameter  $\epsilon wN/\delta$  (product of the equivalent weight flow and rotational speed) with turbine speed and total-pressure ratio as parameters. The efficiency contours are also included. The design work and speed are indicated by point A, whereas design work and equivalent weight-flow parameter are indicated by point B. A comparison of the abscissas of these two points shows that 95 percent design weight flow or an equivalent weight flow of 14.5 pounds per second was passed at design speed. Point A also indicates that the turbine limiting-loading point is reached before design work is extracted. Limiting loading is defined as that point where changes in total-pressure ratio result in no additional change in work output.

Although the actual weight flow of 14.5 pounds per second is in close agreement with the choking weight flow of 14.7 obtained from the analysis in reference 2, it must be remembered that there are certain factors affecting this agreement such that a direct comparison should not be made. Certain phenomena such as viscous effects, boundary-layer buildup, and pressure variations across the channel which reduce the actual weight flow were ignored in the theoretical analysis. Conversely, if the rotor choked and the nozzle-exit tangential velocities were not obtained, the total conditions relative to the rotor would be increased, and the choking weight flow through the rotor would correspondingly increase to a point where close agreement could be obtained.

The limiting-loading condition and peak-efficiency region at design speed are illustrated more clearly in figure 6. The variation in equivalent work and efficiency with total-pressure ratio is shown at design speed. It can be seen that the turbine limiting-loading point is reached at a work output just below design work. A high-efficiency region of 84 percent can be observed at a pressure ratio of 1.65 and about 75 percent design work.

Effect of rotor choking on turbine performance. - The experimental investigation showed that the rotor limited the weight flow before the desired nozzle-exit tangential velocities were obtained. This phenomenon is illustrated in figure 7. The total-to-static pressure ratio across the nozzles at the inner and outer wall is shown as a function of the total-pressure ratio across the turbine at design speed. Beyond a total-pressure ratio of 1.8, there is no change in the total-to-static pressure ratio across the nozzles. Thus, the rotor must be choking such that an increase in total-pressure ratio does not affect the rotor inlet conditions.

It can be seen from figure 6 that at a total-pressure ratio of 1.8, 80 percent design work was extracted at an efficiency near 84 percent. Because the inlet tangential velocity remains constant beyond this pressure ratio (fig. 7), the additional work must be obtained from a change in exit tangential velocity. Figure 6 indicates a large drop in efficiency from the peak as the total-pressure ratio is increased. Since the rotor inlet conditions do not change, the additional losses at the higher pressure ratios must be incurred downstream of the rotor choking region.

The absolute discharge flow-angle survey at the turbine exit is shown in figure 8 for total-pressure ratios of 1.68, 1.98, and 2.54 at design speed. Approximately  $20^\circ$  of undeturning occurred along the major portion of the blade height at a total-pressure ratio of 1.68 and indicated considerable positive exit tangential velocity at the peak efficiency point where a constant rotor-inlet condition was approached.

At a pressure ratio of 1.98, the turbine-exit flow direction was close to axial near the inner wall and approached a positive angle of  $15^{\circ}$  near the outer wall. The decrease in discharge angle resulted in an additional 4 Btu of work per pound of air at a drop of 3 percent in efficiency (indicated by fig. 6). The rotor discharge angle survey at a total-pressure ratio of 2.54 indicates that the turbine-exit flow direction near the outer wall approaches axial, whereas considerable negative tangential velocities near the inner wall are indicated by a negative flow angle in this region. Hence, an increased work, although still slightly less than design work, was extracted at this pressure ratio because of an increased work output near the inner wall.

Possible modification of present design. - The experimental performance of the turbine designed to drive a supersonic compressor indicates that in an attempt to decrease the stress of the rotor hub by use of high turbine-exit absolute velocities, an extreme blade taper, and an insweep of the inner wall, a flow area was used within the rotor that proved insufficient to pass the required weight flow. This, in turn, resulted in nozzle-exit tangential velocities less than design. Thus, design specific work could be obtained only by increasing the total-pressure ratio with resulting negative exit tangential velocities. The turbine performance shows that the limiting-loading point was reached at a work output slightly less than design.

Possible modifications of the present configuration could be made in an attempt to unchoke the rotor. The nozzle flow area could be reduced so that the flow is limited by the nozzles. It would be expected that this modification would result in nozzle-exit tangential velocities approaching design. Under this condition the required specific work would be obtained at a total-pressure ratio below that corresponding to limiting loading. However, in order to obtain the desired weight flow as well as specific work, redesign of the rotor inner wall to increase the flow area would be necessary, as indicated in reference 2.

#### SUMMARY OF RESULTS

In the design of a turbine to power a supersonic compressor, the problem of high stress and high entrance relation Mach numbers at the rotor blade hub were encountered under the condition of equal compressor and turbine diameters. A high degree of taper was incorporated into the blade design reducing the average blade stress at the hub to approximately 46,600 pounds per square inch. The resulting hub and tip solidities were 2.2 and 0.8, respectively. The turbine diameter was increased 8 percent over that of the compressor to reduce the relative Mach number at the rotor hub to 0.69.

In the attempt to decrease the stress at the rotor blade hub by use of high turbine-exit absolute velocities, an extreme blade taper, and an insweep of the inner wall, a flow area was used within the rotor that proved insufficient to pass the desired weight flow. The performance of a 14-inch cold-air model of this configuration indicated that at design speed 95 percent design weight flow was passed. This, in turn, resulted in nozzle-exit tangential velocities less than design. An increase in work could therefore be obtained only with negative exit tangential velocities. However, the turbine limiting-loading point was reached at a work output slightly less than design.

Lewis Flight Propulsion Laboratory  
National Advisory Committee for Aeronautics  
Cleveland, Ohio

## APPENDIX A

## SYMBOLS

The following symbols are used in this report:

A <sub>a</sub>	annular area, sq ft
A <sub>f</sub>	frontal area, sq ft
C	constant of proportionality
c <sub>p</sub>	specific heat at constant pressure, Btu/(lb)(°R)
c <sub>v</sub>	specific heat at constant volume, Btu/(lb)(°R)
D	diameter, ft
g	acceleration due to gravity, 32.17 ft/sec <sup>2</sup>
h	specific enthalpy, Btu/lb
K	constant equal to $2g \frac{\gamma}{\gamma-1} R$ , sq ft/(sec <sup>2</sup> )(°R)
M	Mach number
N	rotational speed, rpm
p	absolute pressure, lb/sq ft
R	gas constant, ft°R
r	radius, ft
s <sub>b</sub>	unit blade stress, lb/sq in.
T	absolute temperature, °R
U	blade velocity, ft/sec
V	gas velocity, ft/sec
v <sub>cr</sub>	critical velocity defined as gas velocity at Mach number of 1, ft/sec
w	relative gas velocity, ft/sec

w weight-flow rate, lb/sec

$\alpha$  flow angle of absolute velocity measured from axial direction, deg

$\gamma$  ratio of specific heats,  $c_p/c_v$

$\Delta$  prefix to indicate change

$\delta$  ratio of inlet-air pressure to NACA standard sea-level pressure,

$$\frac{p_i}{p^*}$$

$\epsilon$  function of  $\gamma$ ,  $\frac{\gamma^*}{\gamma} \left[ \frac{\left(\frac{\gamma+1}{2}\right)^{\frac{\gamma}{\gamma-1}}}{\left(\frac{\gamma^*+1}{2}\right)^{\frac{\gamma^*-1}{\gamma^*-1}}} \right]$

$\eta$  adiabatic efficiency defined as ratio of turbine work based on temperature measurements to ideal turbine work based on inlet total conditions, and outlet total pressure consisting of static pressure plus pressure head corresponding to axial component of velocity

$\theta_{cr}$  squared ratio of critical velocity at turbine inlet to critical velocity at NACA standard sea-level temperature  $\left( \frac{V_{cr}}{V_{cr}^*} \right)^2$

$\rho$  gas density, lb/cu ft

$\rho_m$  blade metal density, lb/cu ft

$\psi$  blade stress correction factor

$\omega$  angular velocity, radians/sec

## Subscripts:

h rotor hub or inner radius

i turbine inlet

r relative to rotor

t rotor tip or outer radius

- u tangential component
- x axial component
- 1 measuring station upstream of nozzles
- 2 measuring station at nozzle outlet, rotor inlet
- 3 measuring station downstream of rotor
- 4 measuring station in outlet pipe

Superscripts:

- \* NACA standard conditions
- ' total state

## APPENDIX B

## DERIVATION OF EQUATION TO CALCULATE OUTLET TOTAL PRESSURE

The outlet total pressure used for rating the turbine has been defined as containing the static pressure and the pressure head corresponding to the axial component of outlet velocity. This total pressure was calculated from the static pressure, weight-flow rate, flow area, and absolute flow angle from the energy equation, the equation of continuity, and the equation of state. The derivation of the equation is as follows: The relations

$$V_{x,3} = \frac{w}{\rho_3 A_{a,3}} \quad (B1)$$

and

$$\rho_3 = \frac{p_3}{RT_3} \quad (B2)$$

were obtained from the continuity equation and the equation of state.

Since  $T'_3 = T'_4$  by assumption and  $\frac{V_{x,3}}{\cos \alpha_3} = V_3$  by definition, the energy equation can be written as

$$T_3 = T'_4 - \frac{V_{x,3}^2}{2g \frac{r}{r-1} R \cos^2 \alpha_3} \quad (B3)$$

By the substitution of (B3) into the equation of state (B2) the unknown  $T_3$  is eliminated and the equation

$$\rho_3 = \frac{p_3}{R \left( T'_4 - \frac{V_{x,3}^2}{2g \frac{r}{r-1} R \cos^2 \alpha_3} \right)} \quad (B4)$$

is obtained. For simplicity,  $2g \frac{r}{r-1} R$  was set equal to a constant  $K$ .

The equation (B4) was substituted into the continuity equation (B1) to eliminate the unknown  $\rho_3$  and to obtain the equation

$$V_{x,3} = \frac{wR}{A_{a,3} p_3} \left( T'_4 - \frac{V_{x,3}^2}{K \cos^2 \alpha_3} \right)$$

from which, by rearrangement, was obtained

$$V_{x,3}^2 + V_{x,3} \frac{p_3 A_{a,3}}{wR} K \cos^2 \alpha_3 - T_4' K \cos^2 \alpha_3 = 0$$

When the preceding quadratic equation is solved for  $V_{x,3}$ , it becomes

$$V_{x,3} = \frac{-\frac{p_3 A_{a,3}}{wR} K \cos^2 \alpha_3 + \sqrt{\left(\frac{p_3 A_{a,3}}{wR} K \cos^2 \alpha_3\right)^2 + 4T_4' K \cos^2 \alpha_3}}{2} \quad (B5)$$

The ratio of total pressure to static pressure can be defined as

$$\left(\frac{p_3'}{p_3}\right)^{\frac{\gamma-1}{\gamma}} = 1 + \frac{V_{x,3}^2}{K T_3} \quad (B6)$$

By using the continuity relation

$$\rho_3 = \frac{w}{V_{x,3} A_{a,3}}$$

the density  $\rho_3$  can be eliminated from the equation of state

$$T_3 = \frac{p_3}{R \rho_3} = \frac{p_3 A_{a,3} V_{x,3}}{R w} \quad (B7)$$

After equation (B7) is substituted into (B6) to eliminate the static temperature  $T_3$ , the equation is obtained

$$\left(\frac{p_3'}{p_3}\right)^{\frac{\gamma-1}{\gamma}} = 1 + \frac{V_{x,3} R w}{K p_3 A_{a,3}} \quad (B8)$$

The velocity term  $V_{x,3}$  is eliminated by substituting equation (B5) into (B6), which results in the equation

$$\left(\frac{p'_3}{p_3}\right)^{\frac{r-1}{r}} = 1 + \frac{Rw}{2Kp'_3 A_{a,3}} \left[ -\frac{p_3 A_{a,3} K \cos^2 \alpha_3}{wR} + \sqrt{\left(\frac{p_3 A_{a,3} K \cos^2 \alpha_3}{wR}\right)^2 + 4T'_4 K \cos^2 \alpha_3} \right]$$

which, when simplified, becomes

$$\left(\frac{p'_3}{p_3}\right) = \left[ 1 - \frac{1}{2} \cos^2 \alpha_3 + \frac{1}{2} \sqrt{\cos^4 \alpha_3 + \left(\frac{Rw}{p'_3 A_{a,3}}\right)^2 \frac{4T'_4}{K} \cos^2 \alpha_3} \right]^{\frac{r}{r-1}} \quad (B9)$$

Equation (B9) was the equation used to calculate outlet total pressure.

#### REFERENCES

1. LaValle, Vincent L., and Huppert, Merle C.: Effects of Several Design Variables on Turbine-Wheel Weight. NACA TN 1814, 1949.
2. Stewart, Warner L.: Analytical Investigation of Flow Through High-Speed Mixed-Flow Turbine. NACA RM E51H06, 1951.
3. Heaton, Thomas R., Slivka, William R., and Westra, Leonard F.: Cold-Air Investigation of a Turbine with Nontwisted Rotor Blades Suitable for Air Cooling. NACA RM E52A25, 1952.
4. Kohl, Robert C., Herzig, Howard Z., and Whitney, Warren J.: Effects of Partial Admission on Performance of a Gas Turbine. NACA TN 1807, 1949.

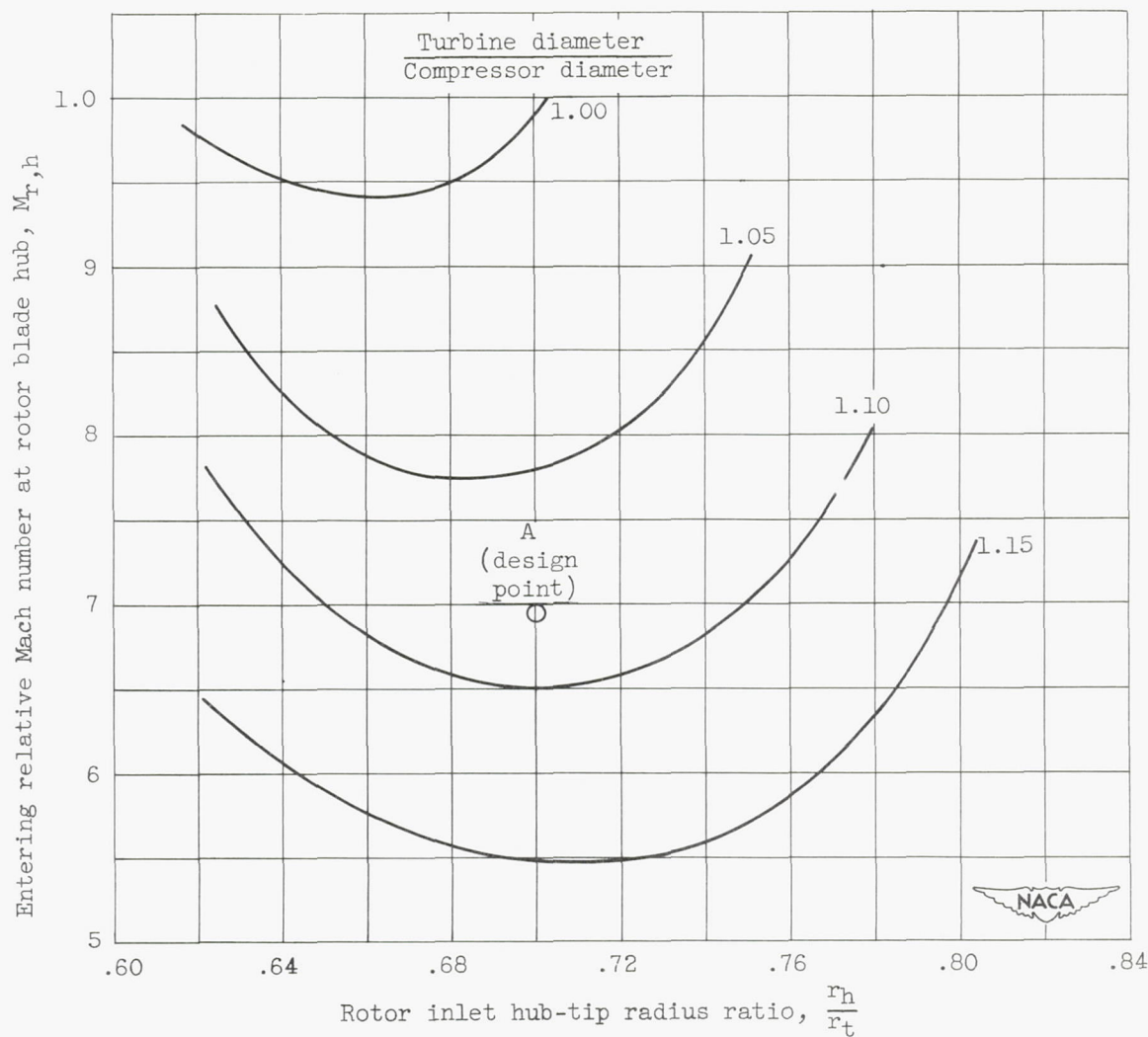


Figure 1. - Variation of relative Mach number at rotor blade hub with hub-tip radius ratio for various turbine-to-compressor diameter ratios.  
Compressor equivalent specific air weight flow, 30 pounds per second per square foot; compressor tip speed, 1500 feet per second.

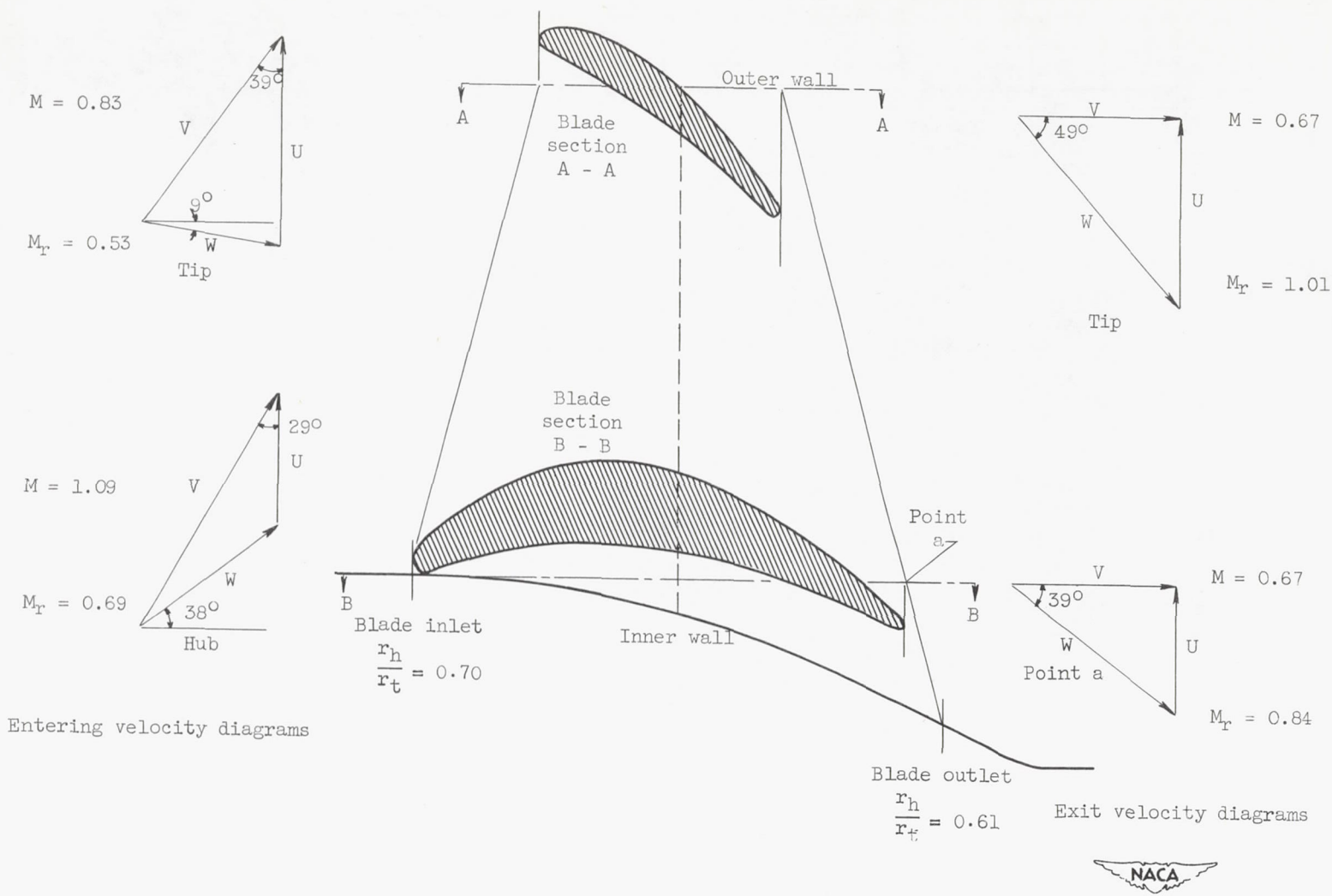


Figure 2. - Rotor blade sections and velocity diagrams.

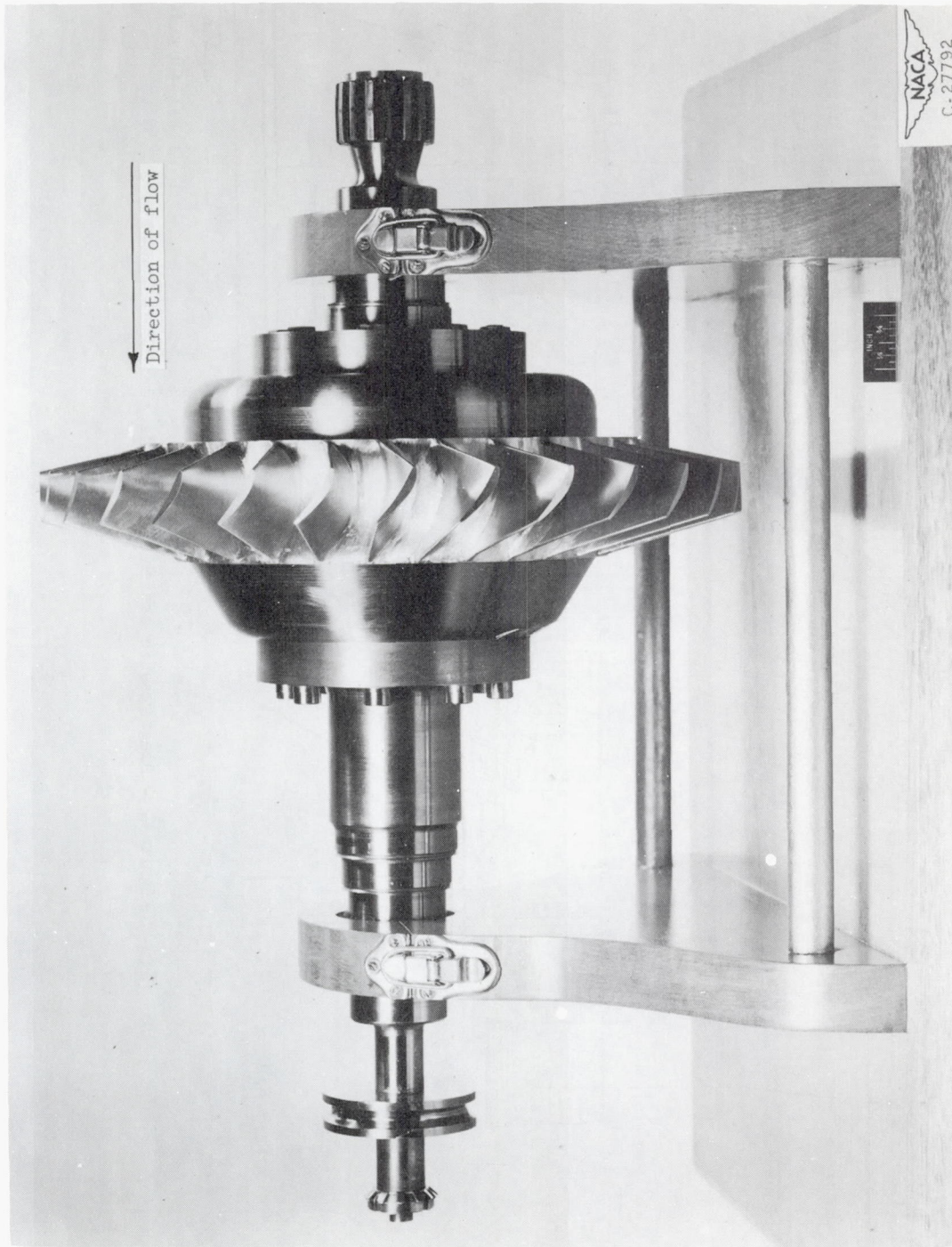


Figure 3. - Side view of turbine rotor assembly.

M E52C25

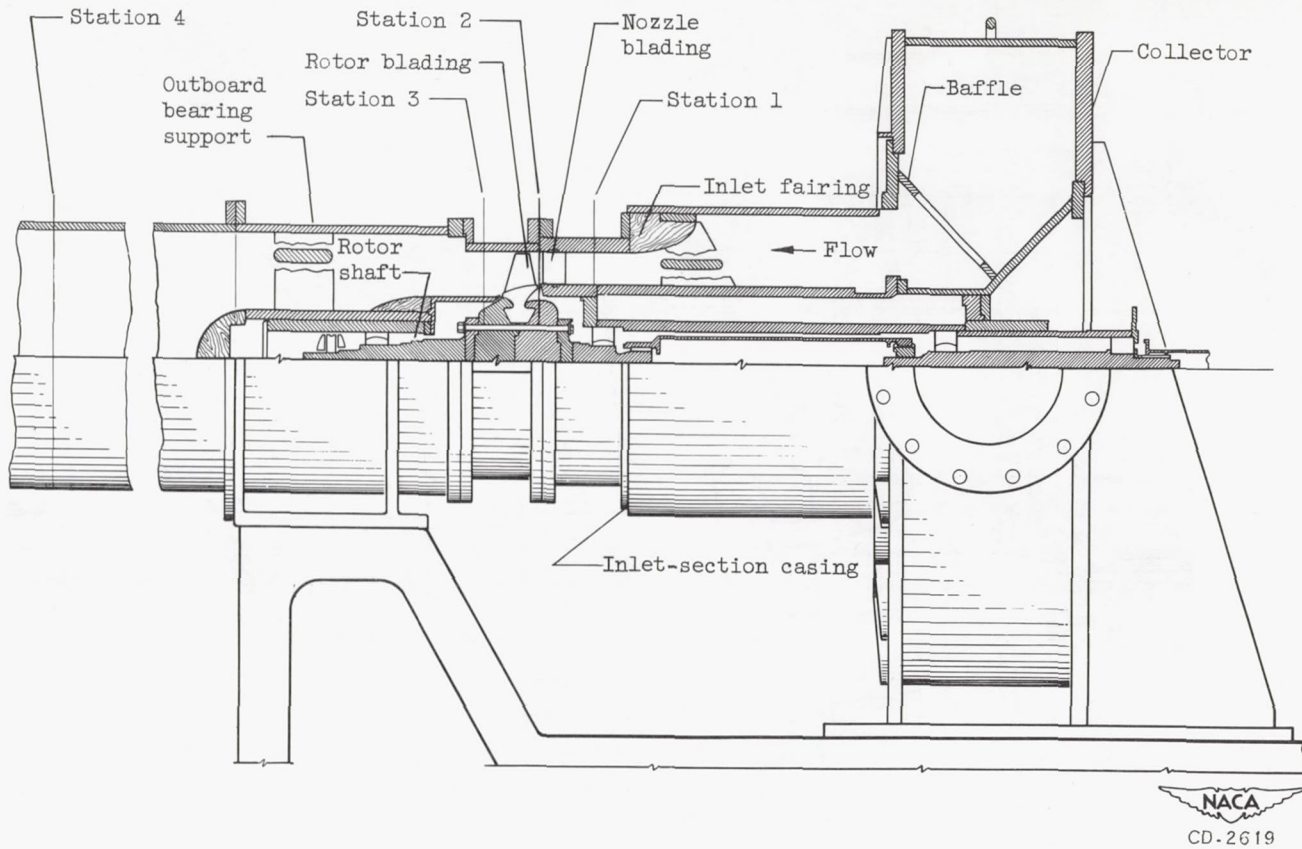


Figure 4. - Diagrammatic sketch of cold-air turbine test section.

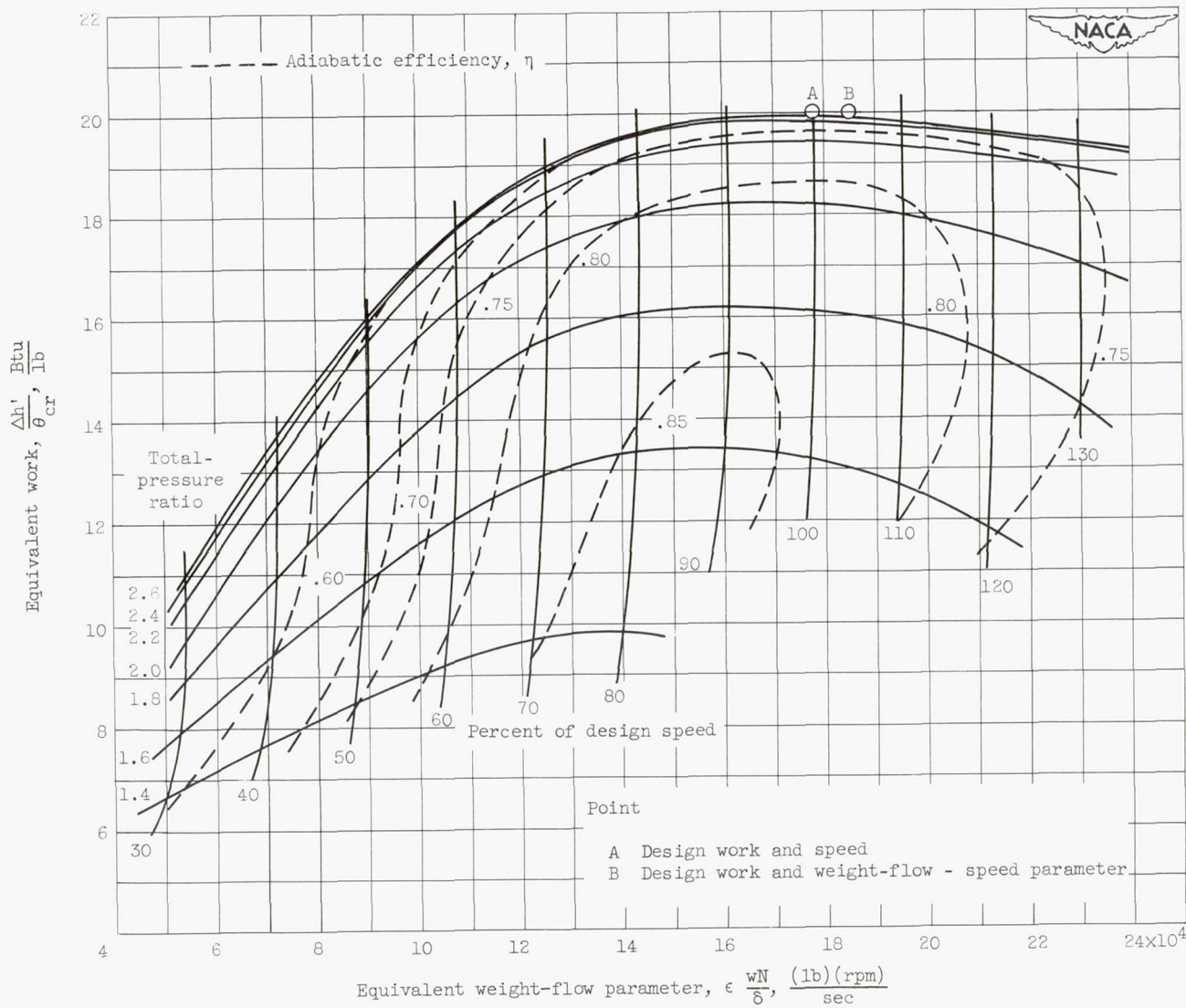


Figure 5. - Over-all performance of turbine.

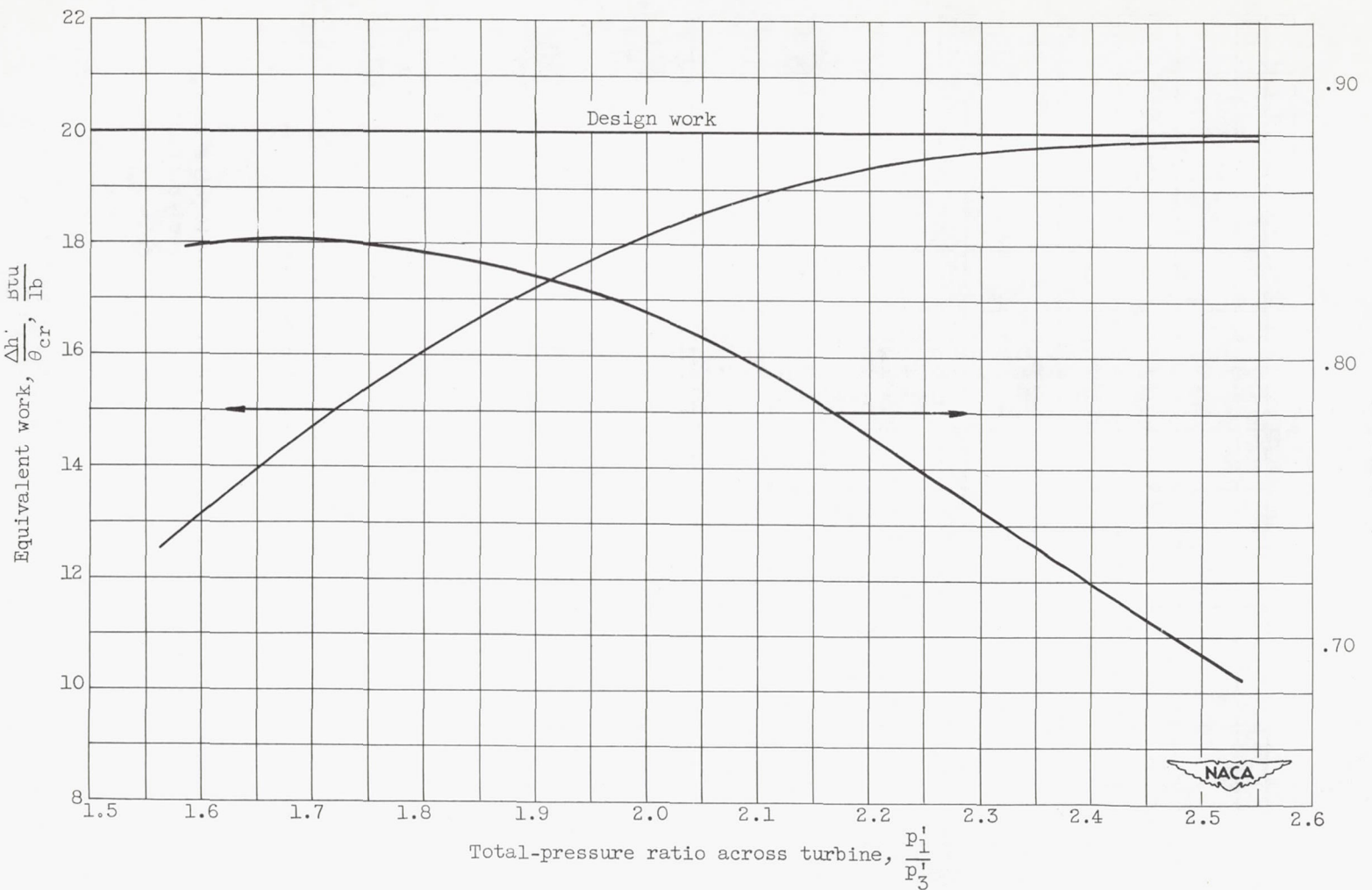


Figure 6. - Variation in equivalent work and efficiency with total-pressure ratio across turbine at design speed.

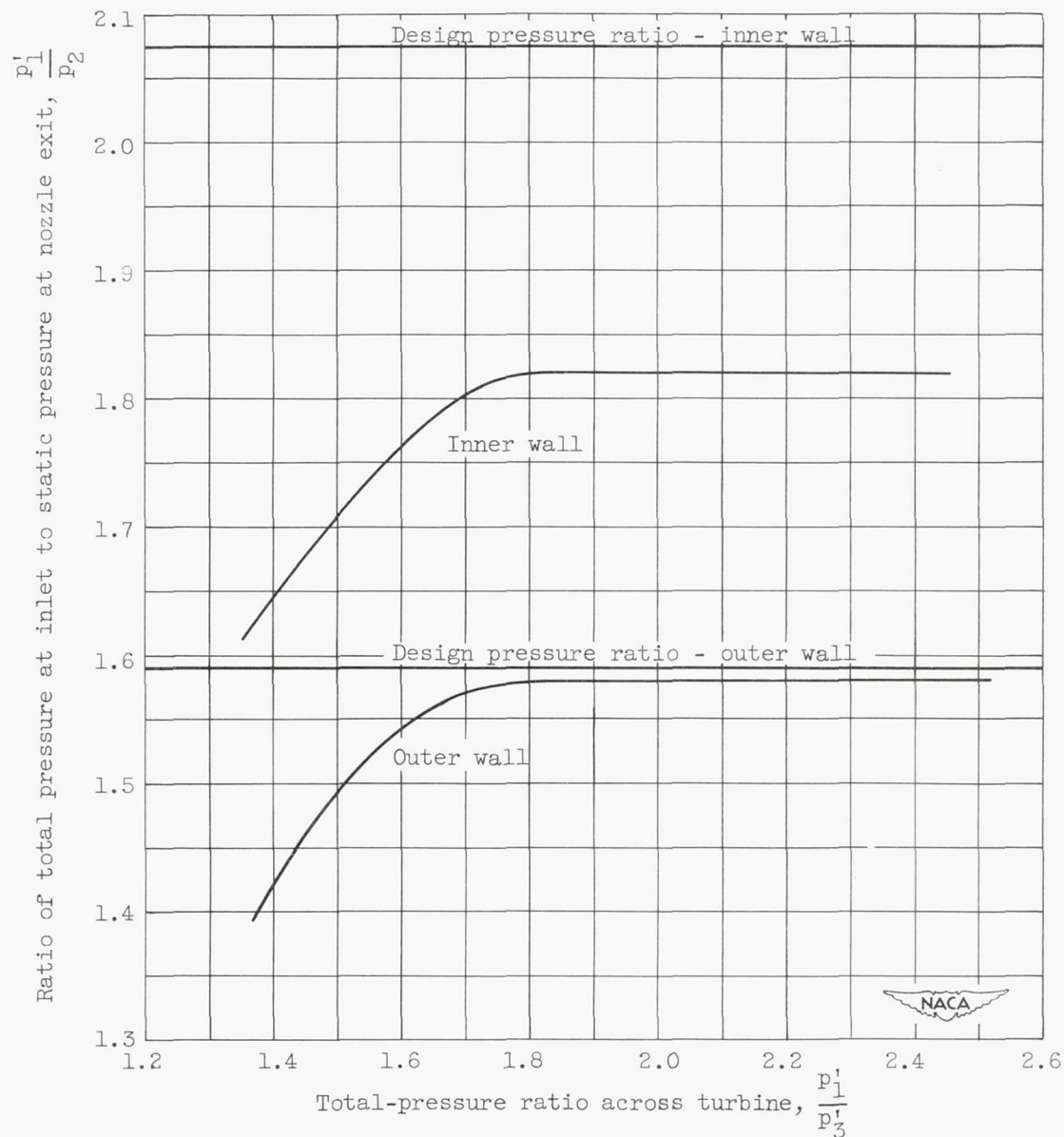


Figure 7. - Effect of total-pressure ratio across turbine on total-to-static pressure ratio across nozzles at design speed.

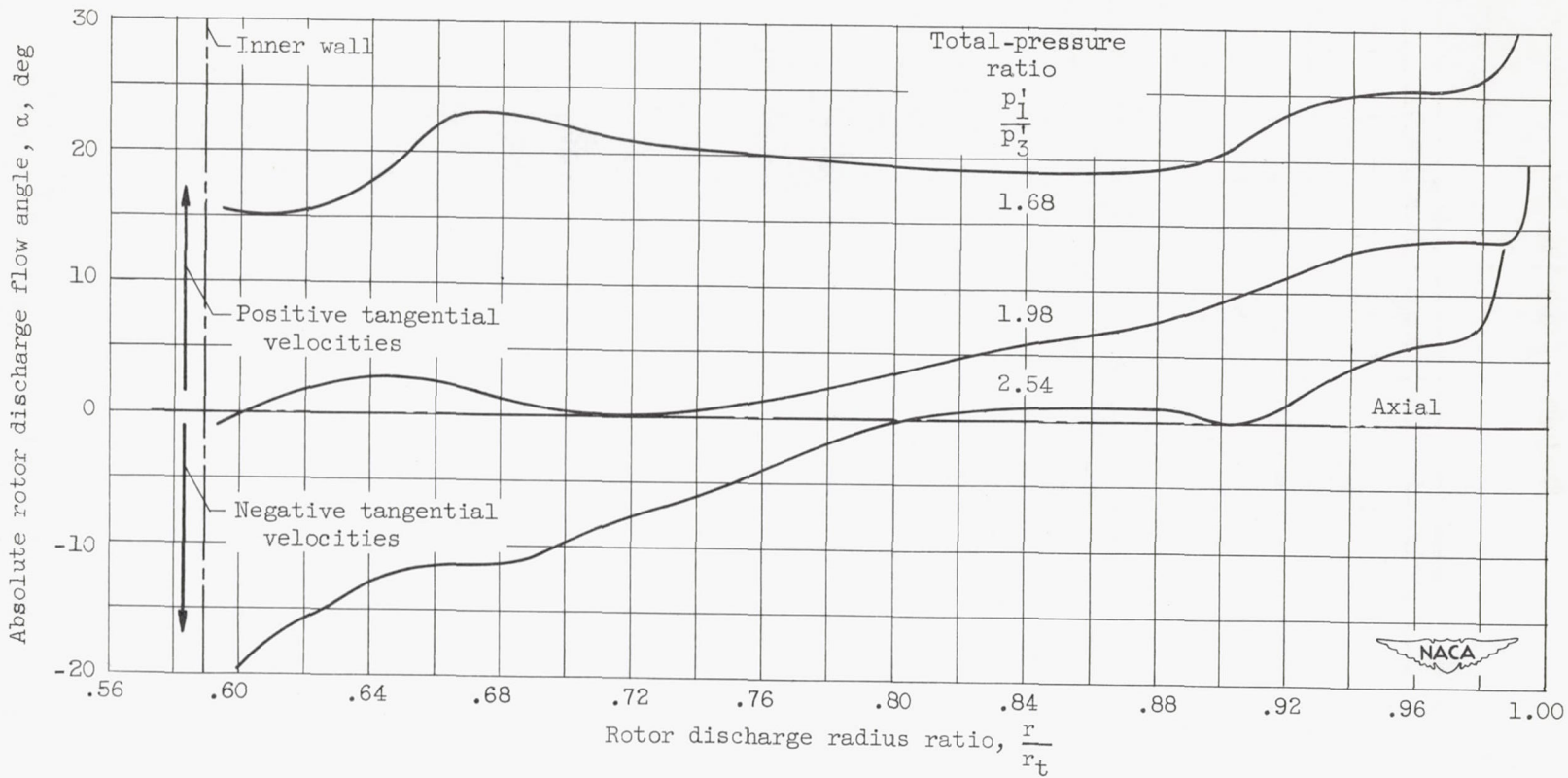


Figure 8. - Variation of rotor discharge flow angle with rotor discharge radius ratio for several turbine operating pressure ratios at design speed.